Ring-down gravitational waves and lensing observables: How far can a wormhole mimic those of a black hole?

Kamal K. Nandi, Ramil N. Izmailov, Almir A. Yanbekov, and Azat A. Shayakhmetov

Zel'dovich International Center for Astrophysics, Bashkir State Pedagogical University, 3A, October Revolution Street, Ufa 450000, Republic of Bashkortostan, Russia
(Received 7 November 2016; revised manuscript received 20 March 2017; published 9 May 2017)

It has been argued that the recently detected ring-down gravity waveforms could be indicative only of the presence of light rings in a horizonless object, such as a surgical Schwarzschild wormhole, with the frequencies differing drastically from those of the horizon quasinormal mode frequencies ω_{QNM} at late times. While the possibility of such a horizonless alternative is novel by itself, we show by the example of the Ellis-Bronnikov wormhole that the differences in ω_{QNM} in the eikonal limit (large l) need not be drastic. This result will be reached by exploiting the connection between ω_{QNM} and the Bozza strong field lensing parameters. We shall also show that the lensing observables of the Ellis-Bronnikov wormhole can be very close to those of a black hole (say, SgrA* hosted by our galaxy) of the same mass. This situation indicates that the ring-down frequencies and lensing observables of the Ellis-Bronnikov wormhole can remarkably mimic those of a black hole. The constraint on wormhole parameter γ imposed by experimental accuracy is briefly discussed. We also provide independent arguments supporting the stability of the Ellis-Bronnikov wormhole proven recently.

I. INTRODUCTION

Direct detection of gravity waves that originated 1.4 billion years ago from a binary merger is one of the great discoveries of this century [1,2], once again confirming Einstein's theory of gravity. The detected waves are assumed to contain the signatures of quasinormal modes (QNM) characteristic of the formation of a final black hole horizon. Theoretically, these modes are resonant nonradial deformations induced by external perturbations and are dictated strictly by the boundary conditions at the horizon, with the Schwarzschild horizon remaining stable under external perturbations. For the first time, an alternative source of such waves has been proposed by Cardoso *et al.* [3], which is a horizonless, static surgical Schwarzschild thin-shell wormhole joined at the throat $r_0 > 2M$.

However, the surgical wormhole risks collapse to a point $r_0 = 0$ under perturbations caused by a moving particle destroying the unstable photon spheres at $r = 3M$. Because of the negative unbound potential of the problem, the throat would at best be metastable against collapse to $r_0 = 0$ and at worst, if the joining surface is a classical membrane, be completely unstable [4]. Granting that the radial test particle motion somehow causes nonradial deformations of spacetime needed for QNM emission, stability of the surgical wormhole against such perturbations remains a "completely uncharted territory" [4].

Stability issues aside, the drastic difference, concluded in [3], in the fundamental ring-down frequencies between the surgical wormhole and a black hole of the same mass M seems to highlight the topological differences between a throat and a horizon. We shall exemplify that the difference need not always be drastic—there could be situations

where wormhole ring-down modes in the eikonal limit could be very close to those of a black hole of the same mass. To this end, we note that Jordan frame Brans solutions can represent wormholes and naked singularities [5], but never black holes, as has been reported recently by Faraoni *et al.* [6]. We here add that their conclusion holds true as long as the relevant parameter of the Brans wormhole solution assumes *real* values as opposed to imaginary ones (meaning that a throat is not topologically changing to a horizon). If the parameter takes on an *imaginary* value, the black hole solution with a vanishing scalar field could result, but several arguments in Sec. V indicate that such an end state is unlikely to occur in practice. As an example, note that the Brans II solution can be rephrased in the Einstein conformal frame as what is (not widely) known as the horizonless regular Ellis-Bronnikov wormhole [7,8]. It does not represent a black hole for real values of parameters but does so for an imaginary value, which is unreachable from a real regime. Therefore, we should regard the wormhole as an independent entity by itself that is distinct from a black hole of the same mass.

With regard to the ring-down modes, Konoplya and Zhidenko [9] very recently studied the dominating low l modes in the gravitational radiation.[1] They showed that (i) the $l = 2$ ($n = 0$) mode $q\omega = 1.246 - 0.192i$ of the Ellis-Bronnikov wormhole has different quality factor $\sim \text{Re}(\omega)/\text{Im}(\omega)$ from that of the Schwarzschild black hole

---

[1] We thank R. A. Konoplya and A. Zhidenko for pointing out in private correspondence the similarity of the problem they dealt with in their paper, especially the late-time behavior of the gravitational radiation.

for which $M\omega = 0.3737–0.0890i$. This means that one can always differentiate a wormhole from a spherically symmetric black hole in general relativity, even if the corresponding mass parameters, q and M, are unknown. (ii) The *late-time behavior* of ring-down modes for the $l = 2$ axial gravitational perturbations of the Ellis-Bronnikov wormhole with scalar field mass $q = 2.16M$ shows the same decay rate as that of a Schwarzschild black hole of mass M but higher oscillation frequency and finally (iii) the wormhole, despite the different behavior of the effective potential compared to that of the black hole, either rings as a black hole at all times or rings differently also at all times, depending on the chosen values of its parameters. In the large l limit, however, it will turn out that the wormhole and black hole modes of ω_{QNM} are almost, but not exactly, the same. In an earlier work, Konoplya and Zhidenko [10] developed generic formulas for ω_{QNM} in the low l limit for the Morris-Thorne wormhole, static and rotating, using the Wentzel–Kramers–Brillouin (WKB) method.

The purpose of this paper is to consider the analytic (as opposed to surgical) horizonless Ellis-Bronnikov wormhole and compare its practically observable properties with those of a Schwarzschild black hole to see how far they tally with each other. We shall show that the quantitative deviations in the large l limit of ω_{QNM} and strong field Bozza lens parameters [11] between the SgrA* and Ellis-Bronnikov wormhole need not be too drastic, indicating that the latter can very well observationally mimic the black hole. The precision required to distinguish between the two types of objects imposes a constraint on the wormhole parameter. Some arguments supporting the recently proven stability of the Ellis-Bronnikov wormhole are also provided.

We wish to emphasize that we are considering a static compact object merely as a toy model for SgrA* as has been considered, for instance, by Lacroix and Silk [12], where they commented that a spinning object would be more appropriate. The reason is that many astrophysical observations of black holes are not consistent with the static Schwarzschild metric. For instance, the detection of 106-day radio variability in the $\lambda > 1$ cm emission from SgrA* signals a small spin ($a \simeq 0.088M$) [13] that could lead to new physical phenomenon like superradiance [14]. Additionally, the eikonal limit of Kerr QNMs is not yet fully understood (see the review in [15]). Given these complications, the results of the present paper, though limited by the assumption of staticity, could nevertheless be useful from the heuristic point of view.

In Sec. II, we review the Ellis-Bronnikov wormhole including its Schwarzschild limit. In Sec. III, we quantitatively compute QNM frequencies using strong field wormhole lensing. In Sec. IV, lensing observables are calculated, and a constraint on the wormhole parameter is obtained. In Sec. V some arguments supporting the recently proven stability of the Ellis-Bronnikov wormhole. Section VI concludes the paper. We choose units such that $8\pi G = 1$, $c = 1$ unless specifically restored.

II. ELLIS-BRONNIKOV WORMHOLE

We start with the Einstein field equations that follow from the action with a minimally coupled scalar field ϕ. The action and the resulting field equations are

$$S = \int \sqrt{-g}d^4x[R - \varepsilon g^{\mu\nu}\phi_{,\mu}\phi_{,\nu}], \tag{1}$$

$$R_{\mu\nu} = \varepsilon\phi_{,\mu}\phi_{,\nu}, \tag{2}$$

$$\Box\phi \equiv \phi_{;\mu}^{;\mu} = 0, \tag{3}$$

where ε is a constant, $\phi_{,\mu} \equiv \partial\phi/\partial x^\mu$, and the semicolon denotes a covariant derivative with respect to $g_{\mu\nu}$. The source scalar field ϕ is assumed to be a ghost field, defined by $\varepsilon = -1$, that violates all energy conditions. The Ellis-Bronnikov wormhole solution of Eqs. (2) and (3) is given by [7,8]

$$d\tau_{\mathrm{EB}}^2 = Adt^2 - Bd\ell^2 - C(d\theta^2 + \sin^2\theta d\varphi^2)], \tag{4}$$

$$A(\ell) = \exp\left[-\pi\gamma + 2\gamma\tan^{-1}\left(\frac{\ell}{m_0}\right)\right], \tag{5}$$

$$B(\ell) = A^{-1}(\ell), \qquad C(\ell) = B(\ell)(\ell^2 + m_0^2), \tag{6}$$

$$\phi(\ell) = \kappa\left[\frac{\pi}{2} \pm 2\tan^{-1}\left(\frac{\ell}{m_0}\right)\right], \qquad 2\kappa^2 = 1 + \gamma^2, \tag{7}$$

where $\ell \in (-\infty, \infty)$, and m_0 and γ are arbitrary constants of integration. This horizonless, traversable, everywhere regular wormhole for real values of $\gamma > 0$ has manifestly two asymptotically flat regions, one with positive Keplerian mass $M (= m_0\gamma)$ and the other with negative mass $-Me^{\pi\gamma}$, situated on either side of a regular throat at $\ell_{\mathrm{th}} = M$. The throat radius is obtained by minimizing the areal radius, or from $dC/d\ell = 0$. The photon sphere is defined by the positive root of

$$\frac{A'}{A} = \frac{C'}{C}, \tag{8}$$

where primes denote differentiation with respect to ℓ. Thus, the photon sphere appears at $\ell_{\mathrm{ps}} = 2M$. Without loss of rigor, we henceforth regard $M > 0$, together with the constant $\gamma > 0$, as independent arbitrary parameters of the solution. Studying circular null geodesics, Cardoso *et al.* [16] in an earlier work showed that the QNM frequencies of a black hole in the eikonal limit ($l \gg 1$), restoring c and retaining their notation, is

$$\omega_{\mathrm{QNM}} = \Omega_m l - i\left(n + \frac{1}{2}\right)|\lambda|, \tag{9}$$

$$\Omega_m = c\sqrt{\frac{A_m}{C_m}}, \qquad \lambda = c\sqrt{\frac{A_mC_m'' - A_m''C_m}{2B_mC_m}}, \tag{10}$$

$$A_m \equiv A(\ell_{\text{ps}}), \qquad C_m \equiv C(\ell_{\text{ps}}), \qquad C' \equiv \frac{dC}{d\ell} \quad \text{etc,}$$

where n and l, respectively, are the number of overtone and angular momentum of the perturbation, Ω_m is the angular velocity of the last circular null geodesic (photon sphere), and λ is the Lyapunov exponent determining the instability time scale. The significance of the subscript m throughout the paper is that the functions are calculated at the *minimum* radial distance that is the radius of the photon sphere.

Stefanov *et al.* [17] connected the QNM coefficients in Eq. (9) with the strong lensing parameters as follows:

$$\Omega_m = \frac{c}{u_m}, \qquad \lambda = \frac{c}{u_m \bar{a}}, \qquad (11)$$

where $\bar{a}$ and the minimum impact parameter of the light rays u_m both appear in the strong field Bozza deflection angle $\alpha(\theta)$ given by

$$\alpha(\theta) = -\bar{a} \ln \left(\frac{\theta D_{\text{OL}}}{u_m} - 1 \right) + \bar{b}, \qquad (12)$$

$$\bar{a} = \frac{\Omega_m}{\lambda}, \qquad u_m = \sqrt{\frac{C_m}{A_m}}, \qquad (13)$$

and $\bar{b}$ is another parameter to be found in [11] and calculated explicitly in the Appendix for the Ellis-Bronnikov wormhole, D_{OL} is the observer-lens distance, and θ is the independent angular variable such that θD_{OL} represents the closest approach distance of light rays. The deflection angle logarithmically diverges when the two distances, θD_{OL} and u_m, coincide (meaning photon capture). It can be verified for the Ellis-Bronnikov wormhole (4)–(7) that

$$\bar{a} = 1, \qquad (14)$$

independently of the values of M and γ, sharing the same fundamental property as that of the Schwarzschild black hole. Because of this remarkable sameness, one would be encouraged to know if the Ellis-Bronnikov wormhole has a Schwarzschild limit.

Schwarzschild limit

It seems little known that the Ellis-Bronnikov wormhole (1) reduces analytically, though by no means trivially, to the exact Schwarzschild black hole. This can be shown rigorously as follows: Identify the constant $m_0 = 2B$ in $A(\ell)$ of Eq. (5), and transform $\ell \to r$ by

$$\ell = r - \frac{B^2}{r}, \qquad (15)$$

where $\ell \in (-\infty, \infty)$ now maps to $r \in (0, \infty)$. Then one has $A(\ell) \to P(r) = \exp[-\pi\gamma + 2\gamma\tan^{-1}(\frac{x}{B})]$, where

$x = \frac{1}{2}(r - \frac{B^2}{r})$. Using the identity $\tan^{-1}(\frac{x}{B}) \equiv 2\tan^{-1}(\frac{x+\sqrt{x^2+B^2}}{B}) - \frac{\pi}{2}$, we end up finally with a form of the wormhole solution that happens to be just the Jordan frame Brans Class II solution [18], rewritten in the Einstein frame [19],

$$d\tau_{\text{EB}}^2 \to d\tau_{\text{Brans II}}^2 = P dt^2 - Q dr^2 - R(d\theta^2 + \sin^2\theta d\varphi^2), \qquad (16)$$

$$P(r) = \exp[2\epsilon + 4\gamma\tan^{-1}(r/B)], \qquad (17)$$

$$Q(r) = \left(1 + \frac{B^2}{r^2}\right)^2 \exp[2\zeta - 4\gamma\tan^{-1}(r/B)], \qquad (18)$$

$$R(r) = r^2 Q(r), \qquad (19)$$

$$\phi(r) = \kappa[\pi - 2\tan^{-1}(r/B)], \qquad 2\kappa^2 = 1 + \gamma^2, \qquad (20)$$

where $\epsilon = -\pi\gamma$ and $\zeta = \pi\gamma$ are determined by the condition of asymptotic flatness.

As a first step, we want to know the extent to which the Ellis-Bronnikov wormhole yields post-post-Newtonian (PPN) Schwarzschild values, so we use the identity

$$\tan^{-1}\left(\frac{r}{B}\right) \equiv \frac{\pi}{2} - \tan^{-1}\left(\frac{B}{r}\right), \qquad (21)$$

for $r > 0$, and identifying as before the positive mass of one mouth as $M \ (= m_0\gamma = 2B\gamma)$, it can be verified that the metric functions (17)–(19) admit a Robertson expansion [20] as follows:

$$d\tau_{\text{Brans II}}^2 = \left(1 - 2\alpha_1 \frac{M}{r} + 2\beta_1 \frac{M^2}{r^2} - \frac{3}{2}\xi_1 \frac{M^3}{r^3} + \cdots\right) dt^2$$
$$- \left(1 + 2\gamma_1 \frac{M}{r} + \frac{3\delta_1 M^2}{2r^2} + \frac{\eta_1}{2} \frac{M^3}{r^3} + \cdots\right)$$
$$\times [dr^2 + r^2(d\theta^2 + \sin^2\theta d\varphi^2)], \qquad (22)$$

where the PPN parameters turn out to be

$$\alpha_1 = \beta_1 = \gamma_1 = 1, \qquad \delta_1 = \frac{4}{3} + \frac{1}{3\gamma^2}, \qquad \xi_1 = \frac{8\gamma^2 - 1}{9\gamma^2},$$

$$\eta_1 = \frac{8\gamma^2 + 5}{3\gamma^2}. \qquad (23)$$

Since $\alpha_1 = \beta_1 = \gamma_1 = 1$, the known *weak field* tests cannot distinguish between the Ellis-Bronnikov wormhole and the Schwarzschild black hole as the central gravitating object. To distinguish them, one would require higher order strong field tests that would in principle put constraints on δ_1, ξ_1, and η_1. However, looking at Eqs. (23), it is clear that for real values of γ, there is no way that the parameters may

assume the Schwarzschild values $\delta_1 = \xi_1 = \eta_1 = 1$. The PPN parameters acquire values nearest to, but not the same as, the Schwarzschild values of unity only when $\gamma \to \infty$. To put an observational constraint, say at least on δ_1, hence on γ, one could think about measuring the two-way light deflection $\delta\varphi$ by the Sun up to second order in $\left(\frac{M}{b}\right)$, which for the metric (22) works out to (using the method of Keeton and Petters [21])

$$\delta\varphi \simeq \frac{4M}{b} + \frac{\pi}{4}\left(16 + \frac{1}{\gamma^2}\right)\left(\frac{M}{b}\right)^2, \qquad (24)$$

where b is the impact parameter. Unfortunately, because of unsurmountable technical difficulties, this measurement program has been abandoned [22]. Measuring second order light deflection by the central galactic object is out of the question at this moment. However, it is of interest to note that a constraint on γ can still be imposed from the comparison of the *shadows* of the Schwarzschild black hole and Ellis-Bronnikov wormhole (see Sec. III). Interestingly, the expansion coefficients (23) suggest that, for the exclusive value $\gamma = -i$, it is possible to obtain all the Schwarzschild values: $\alpha_1 = \beta_1 = \gamma_1 = \delta_1 = \xi_1 = \eta_1 = 1$.

The next step is to apply on Eqs. (16)–(20) a combination of inversion, Wick rotation, redefinition of the constant B, and an identity,

$$r = -\frac{B^2}{\rho}, \qquad \gamma = -i, \qquad B = \frac{M}{2\gamma},$$

$$\tanh^{-1}(x) \equiv \frac{1}{2}\ln\left(\frac{1+x}{1-x}\right). \qquad (25)$$

The final outcome is the Schwarzschild metric

$$d\tau^2_{\text{Brans II}} \to d\tau^2_{\text{Sch}}$$

$$= \left(\frac{1 - \frac{M}{2\rho}}{1 + \frac{M}{2\rho}}\right)^2 dt^2 - \left(1 + \frac{M}{2\rho}\right)^4$$

$$\times [d\rho^2 + \rho^2(d\theta^2 + \sin^2\theta d\varphi^2)], \qquad (26)$$

which is what we promised to show.

Returning to the wormhole (16), the radius of the throat and the photon sphere can be obtained as follows: Using $\ell_{\text{th}} = M$ in Eq. (15), we have $r_{\text{th}} - \frac{B^2}{r_{\text{th}}} = M$, from which it follows that the throat appears at the isotropic radius

$$r^{\pm}_{\text{th}} = \frac{M}{2\gamma}\left[\gamma \pm \sqrt{1 + \gamma^2}\right], \qquad (27)$$

but the negative sign has to be discarded as r^-_{th} can become negative for the wormhole range $\gamma > 0$. However, for the black hole value $\gamma = -i$, the throat has a radius $r^{\pm}_{\text{th}} = \frac{M}{2}$. Since $r = \frac{M^2}{4\rho}$, this radius converts to the Schwarzschild horizon $r^{\pm}_{\text{th}} \to \rho_{\text{hor}} = \frac{M}{2}$, as it should. Similarly, using $\ell_{\text{ps}} = 2M$ in Eq. (15), we have $r_{\text{ps}} - \frac{B^2}{r_{\text{ps}}} = 2M$, which yields the

isotropic radius of the photon sphere for the Ellis-Bronnikov wormhole

$$r^{\pm}_{\text{ps}} = \frac{M}{2}\left[2 \pm \sqrt{4 + \frac{1}{\gamma^2}}\right]. \qquad (28)$$

The sign is to be decided by the physical condition that $r^{\pm}_{\text{ps}} > r^{\pm}_{\text{th}} = \frac{M}{2} = 3.12 \times 10^{11}$ cm (for SgrA* mass $M = 4.22 \times 10^6 \ M_{\odot}$; see [23]). For the wormhole, the negative sign has to be discarded as r^-_{ps} can become negative for $\gamma > 0$. Thus, for the wormhole having the mass of SgrA*, one has $r^{+\text{EB}}_{\text{ps}} = 2M = 1.25 \times 10^{12}$ cm, obtained at $\gamma \to \infty$. However, for the black hole value $\gamma = -i$, the photon sphere has a radius $r^{\text{Sch}}_{\text{ps}} = \rho_{\text{ps}} = \frac{M}{2}(2 + \sqrt{3}) = 1.16 \times 10^{12}$ cm $> \frac{M}{2}$, while $r^-_{\text{ps}} < \frac{M}{2}$ is to be discarded. Note that $r^{\pm}_{\text{th}}$ can also be obtained directly from the metric (16) by minimizing its areal radius, and similarly, $r^{\pm}_{\text{ps}}$ by solving Eq. (8).

III. STRONG FIELD LENSING OBSERVABLES

We shall consider the metric (4)–(7) and the latest observed data for the supermassive black hole SgrA* exemplar, believed to be residing at the core of our galaxy, for the computation of strong field lensing observables. The incoming light rays that pass very near to the photon sphere yield strong field lensing observables. For quantitative comparison, the most suitable quantity is [11,12]

$$u_m = D_{\text{OL}}\theta_{\infty}, \qquad (29)$$

where θ_{∞} is the observable angular separation between each set of relativistic images with respect to the central lens. The minimum impact parameter u_m, also called the *radius of the shadow* of the lens, is the central observable to be measured in the currently planned experiments [12]. As is evident from Eqs. (11), the quantitative values of Ω_m and λ depend solely on the strong lensing observable $\bar{a}$, and the minimum impact parameter u_m, and this information alone can already provide distinction between Schwarzschild and Ellis-Bronnikov wormholes. Therefore, we consider situations that guarantee $u_m > \ell_{\text{ps}} = 2M$ for lensed images to be possible, that is, when light is not captured by the photon sphere. We find from the second of Eq. (13) that

$$u^{\text{EB}}_m = \sqrt{\frac{C(\ell_{\text{ps}})}{A(\ell_{\text{ps}})}}$$

$$= M\sqrt{\left(4 + \frac{1}{\gamma^2}\right)\exp\left[2\pi\gamma - 4\gamma\tan^{-1}(2\gamma)\right]}$$

$$= D_{\text{OL}}\theta_{\infty}. \qquad (30)$$

This equation will be used below to constrain the wormhole parameter γ.

Constraint on γ: Experimental situation

It is evident from Eq. (30) that, for $\gamma = -i$, we retrieve just the Schwarzschild value $u_m^{\text{Sch}} = 3\sqrt{3}M$. Our idea is to constrain the real values of γ in u_m^{EB} in such a manner that it approaches u_m^{Sch} as closely as possible in order to support the claim that the Ellis-Bronnikov wormhole could be a black hole mimicker. In this regard, note that the *lowest* value of u_m^{EB} is $2Me$ that appears only at $\gamma \to \infty$. In this case,

$$\frac{u_m^{\text{EB}}}{u_m^{\text{Sch}}} = \frac{2e}{3\sqrt{3}} = 1.04627. \qquad (31)$$

The value of γ can be constrained from below by noting that the angular radius θ_∞ depends only on γ once the mass-to-distance ratio, M/D_{OL}, is provided by independent measurements. Experimental uncertainties in the values of the ratio would induce uncertainties in θ_∞, which in turn would constrain γ.

Let us look at the current experimental situation focusing on the most recent work by Johannsen *et al.* [23]. It is to be noted that, although the realistic situation should involve spin, a final proof of the Kerr nature of black holes is still lacking [23,24], and worse, unlike the static case, a regular spinning wormhole reducing to a Kerr black hole in some limit is a far cry. Further, it has been pointed out in [23] that the central observable, viz., the angular radius θ_∞ of the shadow of a Kerr-like solution (that reduces to the Kerr black hole when the deviation parameters are set to zero), is primarily determined by its mass-to-distance ratio and depends only *weakly* on its spin and inclination. Relying on this weak dependence on spin, we use the simulated mass-to-distance ratio for SgrA* to constrain the real parameter γ of the toy Ellis-Bronnikov wormhole, hopefully without committing errors. For the Kerr-like metric with an assumed spin parameter $a = 0.5M$, Johannsen *et al.* [23] combined the seven-station Event Horizon Telescope (EHT)[2] data at 230 GHz with relevant simulations to obtain the SgrA* mass $M = 4.22 \times 10^6 \, M_\odot$ and its distance $D_{\text{OL}}(= 8.33 \text{ kpc})$. Using these values, we get, from the second in Eq. (30),

$$\theta_\infty^{\text{EB}}(\gamma \to \infty) - \theta_\infty^{\text{Sch}}(\gamma = -i) = 27.253\text{–}26.048$$

$$= 1.205 \text{microarcsec.} \qquad (32)$$

FIG. 1. The function $\Delta(\gamma)$ vs the dimensionless parameter γ.

Since $\theta_\infty^{\text{EB}}(\gamma \to \infty)$ is the lowest value of $\theta_\infty^{\text{EB}}(\gamma)$, the exact difference above cannot be reduced further, which signals the intrinsic difference between the two types of lenses.[3] To find the constraint on γ, we plot, for the above M, the difference function

$$\Delta(\gamma) \equiv \theta_\infty^{\text{EB}}(M, \gamma) - \theta_\infty^{\text{Sch}}(M, \gamma = -i) \qquad (33)$$

against γ to see for what value of γ, Δ becomes closer to 1.205 microarcsec. Figure 1 shows that this happens at $\gamma \geq 80$. This is the desired constraint on γ from below.

The question now is whether the uncertainty in the current level of measurement of θ_∞ is smaller than the difference 1.205 microarcsec just calculated. Once again, based on a reconstructed circular image of SgrA* from a simulated one-day observing run of the EHT array, and employing a Markov Chain Monte Carlo algorithm, Johannsen *et al.* [23] have demonstrated that such an observation can measure the angular radius θ_∞ of the shadow of SgrA* to be (26.4 ± 1.5) microarcsec, i.e., with an uncertainty of 1.5 microarcsec (6%), and that tight constraints on potential deviations from the Kerr metric can be obtained.[4] We see that the current uncertainty 1.5 microarcsec is larger than, but quite close to, the needed accuracy ≤ 1.205 microarcsec. Hence, as of now,

---

[2]The latest EHT, a global network of millimeter-wave very long baseline interferometry (VLBI) array, is expected to provide high-angular-resolution observation of SgrA* and M87. The EHT comprises multiple different telescopes at multiple different sites all over the world. Because the EHT telescopes are so far-flung, the effective size of the telescope is the size of the whole Earth. The shadow of the lens (be it black or a wormhole) is the main observable target in a direct imaging survey, and this is what the EHT collaboration aims to observe in the near future, using the technique of VLBI. The eight observatories comprising EHT are together capable of directly imaging the shadow of the lens. See the site for details: http://www.eventhorizontelescope.org/.
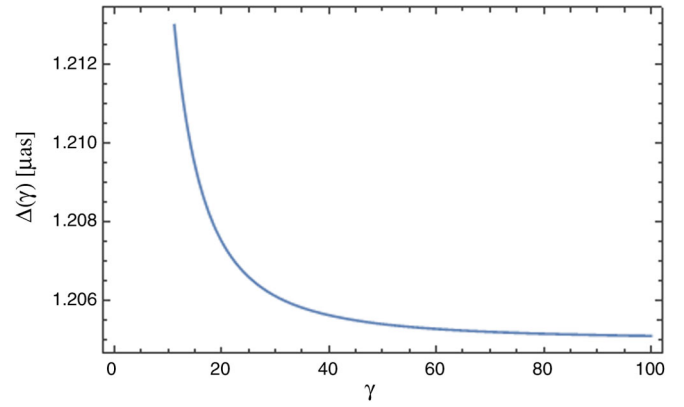
[3]Illustrative numerologies are as follows: $\theta_\infty = (u_m/D_{\text{OL}}) \times (206265 \times 10^6)$ microarcsec. For the Ellis-Bronnikov wormhole of mass $M = 4.22 \times 10^6 \times 1.48 \times 10^5$ cm $= 6.245 \times 10^{11}$ cm, $u_m = 2Me = 3.395 \times 10^{12}$ cm, $D_{\text{OL}} = 8.33 \times 3.085 \times 10^{21} = 2.569 \times 10^{22}$ cm, we have $\theta_\infty^{\text{EB}} = 27.253$ microarcsec. For the Schwarzschild case, $u_m = 3\sqrt{3}M = 3.245 \times 10^{12}$ cm, and similarly $\theta_\infty^{\text{Sch}} = 26.048$ microarcsec.

[4]There appears to be a small gap of 0.36 microarcsec in θ_∞ between the simulated value 26.4 microarcsec for the Kerr-like case and the Schwarzschild value 26.04 microarcsec ($a = 0$). However, this gap is expected to be much reduced since the observed SgrA* spin $a \simeq 0.088M$ is far less than $a = 0.5M$, assumed in [23]. The Kerr lens "identity card" $(\bar{a}, \bar{b}, u_m)$ differs little for $a \approx 0.088M$ from that of the Schwarzschild lens ($a = 0$) as the plots in [25] readily show. Therefore, the value $\theta_\infty^{\text{Sch}} = 26.048$ microarcsec seems quite acceptable at small to moderate spin values.

TABLE I. Bozza lensing observables for Schwarzschild black hole and Ellis-Bronnikov wormhole.

Lens	$\bar{a}$	$\bar{b}$	u_m	r_m	s	$M\omega_{QNM}$ ($n = 0$, $l = 50$)	$\mathrm{Re}(\omega)/\mathrm{Im}(\omega)$
Sch	1	-0.4002	5.196	6.821	0.0321	$9.718 - 0.096i$	101.23
EB	1	-0.4658	5.437	6.821	0.0315	$10.168 - 0.101i$	100.67

measurement of the angular radius of the shadow of our central galactic object cannot distinguish between the types of lenses, but in the near future it should be possible.

We can also calculate other lensing observables defined in [11] such as the separation of images $s^{EB} = \theta_\infty \exp\left[\frac{1}{\bar{a}}(\bar{b} - 2\pi)\right] = 0.0315$, $s^{Sch} = 0.0321$, and the ratio of fluxes $r = \exp\left[\frac{2\pi}{\bar{a}}\right]$ converted to magnitudes $r_m^{EB} = r_m^{Sch} = 2.5 \times \log_{10}(r) = 6.821$. ($\bar{a} = 1$ and for $\bar{b}$, see Appendix).

The zero-mass wormhole ($M = m_0\gamma = 0$) is obtained by putting $\gamma = 0$, $m_0 \neq 0$, which leads to the wormhole metric

$$d\tau_{EB}^2 = dt^2 - d\ell^2 - (\ell^2 + m_0^2)(d\theta^2 + \sin^2\theta d\varphi^2)], \quad (34)$$

$$\phi(\ell) = \frac{1}{\sqrt{2}}\left[\frac{\pi}{2} \pm 2\tan^{-1}\left(\frac{\ell}{m_0}\right)\right] \simeq \text{const} \mp \frac{\sqrt{2}m_0}{\ell}. \quad (35)$$

The constant m_0 is often interpreted as scalar charge *à la* the Wheeleresque mantra "charge without charge" (see [4,26]). In the limit $\gamma \to 0$, the impact parameter $u_m^{EB} \to m_0$, which satisfies $u_m > \ell_{ps} = 0$. Thus, choosing numerical values for m_0 equaling the positive mass of the Ellis-Bronnikov wormhole (which is the SgrA*), we can have exactly the same observables as in Table I. However, it means that the entire mass of SgrA* has to be made up of scalar charges without any molecular structure. This is intriguing but absurd.

IV. QNM FREQUENCIES

Since $\bar{a} = 1$, we can *intuitively* insert the lensing observable u_m in the equation for ω_{QNM} derived using the eikonal limit WKB approximation for the Schwarzschild black hole (for details, see [27]), viz.,

$$\omega_{QNM} = \left(\frac{1}{u_m}\right)\left[\left(l + \frac{1}{2}\right) - \frac{1}{3}\left(\frac{5\alpha^2}{12} - \beta + \frac{115}{144}\right)l^{-1}\right.$$
$$+ \frac{1}{6}\left(\frac{5\alpha^2}{12} - \beta + \frac{115}{144}\right)l^{-2}\bigg]$$
$$- i\alpha\left(\frac{1}{u_m}\right)\left[1 + \frac{1}{9}\left(\frac{235\alpha^2}{432} + \beta - \frac{1415}{1728}\right)l^{-2}\right], \quad (36)$$

where $\alpha \equiv n + \frac{1}{2}$ and $\beta = 0, 1, -3$ for scalar, electromagnetic, and gravitational perturbations, respectively. We noted that the original expression for ω_{QNM} derived in

Eq. (3.1) of [27] had the same form as above except that, in the denominator on the left-hand side, there was the expression $3\sqrt{3}M$ in place of u_m. The surprising thing is that no concept of the radius of the Schwarzschild black hole shadow u_m was used in the WKB method. This led us to guess that a more generic expression for ω_{QNM} should involve u_m in place of the specific Schwarzschild $3\sqrt{3}M$. The motive for this intuitive generalization is the hope that the frequency formula (36) be applicable to any spherically symmetric compact object having a shadow radius u_m (including horizonless wormholes) and remains valid from moderate to large values of l. Then one obtains the ratio of frequencies as

$$\frac{\omega_{QNM}^{Sch}}{\omega_{QNM}^{EB}} = \frac{2e}{3\sqrt{3}} = 1.04627, \quad (37)$$

which is *independent* of γ, β, l, and n. Note that, for $l \gg 1$, one anyway recovers the eikonal approximation (9) and the same ratio of frequencies (37) follow. A consequence of our guesswork is a generic relation from Eqs. (31) and (37), viz.,

$$\omega_{QNM}^{Sch} u_m^{Sch} = \omega_{QNM}^{EB} u_m^{EB} \Rightarrow \omega_{QNM} u_m = \text{complex constant,} \quad (38)$$

indicating that the shadows of the lens contain information on ω_{QNM} and vice versa of any spherically symmetric compact object.

We emphasize that the isotropic form (16) of Ellis-Bronnikov was derived to show its passage to the Schwarzschild black hole, but it is also an equally valid coordinate form. We could do all the calculations of observables using the isotropic form equally well since coordinate choice is a matter of convenience that does not alter the values of actual observables. It can be straightforwardly verified using the isotropic metric (16) that the observables ($\bar{a}$, $\bar{b}$, u_m, r, s, ω_{QNM}) again have exactly the same values. The comparison between SgrA* and the wormhole are summarized at one place in Table I for easy view ($M = 4.22 \times 10^6 \, M_\odot$; the Schwarzschild case has $\gamma = -i$; and the Ellis-Bronnikov case has $\gamma \geq 80$).

V. STABILITY

For the wormhole to be an observationally valid alternative to black holes, the former has to be stable for its very existence. The situation is that, probably due to the inherent

freedom in the choice of perturbation modes, there have been many differing claims in the literature, of which some are mentioned here. Previously, Armendáriz-Picón [28] showed that the massless Ellis-Bronnikov wormhole and at least a nonzero measure set of massive Ellis-Bronnikov wormholes are stable. But it is subsequently argued by González *et al.* [29,30] that the linear stability analysis in [28] applies only to a restricted class of perturbations, which requires the perturbed scalar field to vanish at the throat, $\delta\phi(\ell_{\text{th}}) = 0$. Using numerical simulations, they conclude that the wormhole is unstable under both linear and nonlinear perturbations such that it either expands away to infinity or collapses into the Schwarzschild black hole. The conclusion of instability for the phantom scalar field has been supported also by Bronnikov *et al.* [31].

Below, we point out that, while the emergence of an apparent horizon in the simulation in [30] is an interesting result based on the particular mode of perturbation, the conclusion of the collapse to the black hole seems arguable for the following reasons:

First, González *et al.* [30] take the appearance of the apparent horizon to be a "strong indication" for the formation of an event horizon at a later stage of collapse. Such a hope might be belied since, as they too noted, the apparent horizon is both foliation and observer dependent notion [32]. The main thing is that its existence is not even mandatory for the event horizon. It is quite possible to foliate the Schwarzschild geometry in such a way that there is never any apparent horizon, despite the fact that there is certainly an event horizon [33].

Second, a more recent stability analysis by Novikov and Shatskiy [34] shows that the zero mass wormhole, with the stress decomposed in a clever way, is stable under spherical perturbations (no collapse, no expansion). The stress structure being exactly the same for massive Ellis-Bronnikov wormhole as well,[5] the same analysis can be extended to this case. However, there is a simpler, and mathematical, argument: Note that only the exclusive value of the parameter $\gamma = -i$ in metric (16) yields the exact Schwarzschild black hole, with $\phi = 0$ as was shown. If the wormhole, for which γ must always be *real*, has to really collapse to a black hole, the parameter γ has to jump from a real line into a point on the complex line, augering a sudden topology change. This is absurd, since topology change is against normal experience, at least, on a macroscopic scale [35]. A very recent work by Faraoni *et al.* [6] concludes that Brans solutions cannot collapse into black holes. The Ellis-

Bronnikov wormhole is just such a solution being the Einstein frame variant of the Brans II solution [18], and the same conclusion holds.

Third, we should note that ring-down gravity waves are generated by nonspherical deformations induced by external perturbations. Meanwhile, Bronnikov and Rubin [36] argue that the nonspherical perturbation modes must probably be more stable than the spherical ones, since the effective potential for the perturbations contains centrifugal (and other higher multipoles) barriers, as in the Regge-Wheeler or Zerilli potentials. In fact, stability under nonspherical perturbation is indirectly supported by the negative imaginary part ω_I of the QNM modes as argued in [15,27]. Equation (11) with a positive $\bar{a}$ guarantees that $\lambda > 0$ or $\omega_I < 0$. By the same token, a precise observation of QNM modes would also constitute a test for the existence or otherwise of scalar hair ϕ in the wormhole [15,37].

There exists yet another entirely different window to look at the stability issue, viz., via Tangherlini's approach [38] of "non-deterministic, pre-quantal statistical simulation" of photon motion in a medium yielding reflection (R) and transmission (T) coefficients across a surface in the medium. Taking into account the generic feature in curved space-time, namely, that observations depend on the location of the observer, this approach yields observer-dependent *perception of stability* of the wormhole in terms of these coefficients. While one observer perceives instability, another observer might perceive stability (see, for details, [39]).

VI. CONCLUSIONS

Most of the numerous works on QNM frequencies beginning with the seminal work by Vishveshwara [40] in 1970 until its most recent application to wormholes [3,9] involve spherically symmetric static sources as toy models. However, it is to be remarked that spin is an important factor, and many astrophysical observations of black holes are inconsistent with the Schwarzschild metric.[6] A glimpse of such inconsistency is provided by the observed radio variability in the emission spectrum from SgrA* believed to be induced by a small spin of an assumed Kerr black hole [13]. Nonetheless, studies using static sources provide very useful information on the mode spectrum including the more interesting case of low-lying frequencies ($n = 0$, $l = 2$ is the dominant gravitational wave mode giving the famous $M\omega_{\text{QNM}}^{\text{Sch}} = 0.3737 - 0.0890i$).

Cardoso *et al.* [3] consider a static surgical wormhole (born out of cut-paste surgery joining two copies of Schwarzschild black holes) as a heuristic model that could be extended by including other effects such as spin but, they argue, none of these effects is expected to change the

---

[5]The stress tensor threading the massive Ellis-Bronnikov wormhole has the same decomposable components $\rho = -\frac{m^2(1+\gamma^2)}{(\ell^2+m^2)^2}\exp\left[-\gamma\{\pi - 2\tan^{-1}\left(\frac{\ell}{m}\right)\}\right]$, $p_r = \rho$, $p_\theta = p_\varphi = -\rho$. Both the weak energy condition (WEC), $\rho \geq 0$, and the null energy condition (NEC), $\rho + p_r \geq 0$, are violated. For $\gamma = 0$, one has the stress of the zero mass case decomposed by Novikov and Shatskiy [30].

[6]We thank an anonymous referee for directing our attention to this point and to the question of how it could be constrained by observations.

qualitative picture. The present work has to be regarded as an improvement on the same idea, where the artificial surgical wormhole has been replaced by the regular stable Ellis-Bronnikov wormhole. The latter, being a solution of general relativity with a well defined source, stands a better chance for its occurrence in nature as a competing astrophysical object. This notwithstanding, the results of the present paper should be taken as indicative rather than concrete due to lack of spin. An exact treatment incorporating spin would require a separate follow-up investigation to see if the frequencies emanated from a spinning black hole can be connected with its strong field lensing observables in a manner discovered by Stefanov *et al.* [17] for the static case. It is premature to say if this connection exists at all, but at least the strong field observables for SgrA* with its estimated small spin ($a \simeq 0.088M$) in the Kerr metric do not differ appreciably from their static values ($a = 0$), as the plots of the lens "identity card" ($\bar{a}$, $\bar{b}$, u_m) in [25] show.

The merit of the chosen Ellis-Bronnikov wormhole is that it is observationally indistinguishable from the Schwarzschild black hole in the weak field regime since the PPN parameters are the same ($\alpha_1 = \beta_1 = \gamma_1 = 1$). This result raises the possibility if this wormhole can act as a black hole mimicker beyond PPN approximation. We argue that it can, but only within the experimental accuracy as available today. A better accuracy in the future will certainly distinguish between the two objects. Black hole mimickers are not unknown in the literature. For instance, gravastar models mimicking black holes have been investigated by Chirenti and Rezzolla [41,42]. Once again, unlike artificial gravastars, the Ellis-Bronnikov wormhole is more natural and much simpler. Moreover, it has been shown that the wormhole reduces exactly to the Schwarzschild black hole under the special choice $\gamma = -i$. One would then think that the Ellis-Bronnikov wormhole for different values of *real* γ would lead to observable signatures very different from those of the Schwarzschild black hole obtained at *imaginary* γ. Remarkably, this need *not* be the case. It was shown that the main observable u_m rapidly saturates to $2Me$ at $\gamma \to \infty$, which is indeed not much different from the Schwarzschild value $3\sqrt{3}M$. In this sense, the Ellis-Bronnikov wormhole can be regarded as assuming *an eternal identity* by itself, just like the classical Schwarzschild black hole.

We applied our calculations to the object residing at the center of our galaxy that is speculated to be a black hole (SgrA*) of mass $M = 4.22 \times 10^6 \, M_\odot$ situated at a distance $D_{\mathrm{OL}} = 8.33$ kpc [23]. If instead we regard the object as the Ellis-Bronnikov wormhole, then it turns out that both the objects remarkably share the same value of Bozza strong field lensing parameter, $\bar{a} = 1$. It was further shown that the ratio between the black and wormhole of the same mass with regard to ring-down gravitational wave mode in the eikonal limit is set by $\frac{\omega_{\mathrm{QNM}}^{\mathrm{Sch}}}{\omega_{\mathrm{QNM}}^{\mathrm{EB}}} = \frac{2e}{3\sqrt{3}} = 1.04627$ independently of M, γ, l, and n. This ratio cannot be reduced further as the object either rings as a black hole at all times or rings differently also at all times, depending on the chosen values of its parameters [9]. It was also calculated that $\theta_\infty^{\mathrm{EB}} = 27.253$ microarcsec and $\theta_\infty^{\mathrm{Sch}} = 26.048$ microarcsec, which differ by just 1.205 microarcsec. Other specified observables [11] were also calculated, such as the separation of relativistic images $s^{\mathrm{EB}} = \theta_\infty^{\mathrm{EB}} \exp\left[\frac{1}{\bar{a}}(\bar{b} - 2\pi)\right] = 0.0315$, $s^{\mathrm{Sch}} = 0.0321$, and the ratio of fluxes $r = \exp\left[\frac{2\pi}{\bar{a}}\right]$ converted to magnitudes yields $r_m^{\mathrm{EB}} = r_m^{\mathrm{Sch}} = 2.5 \times \log_{10}(r) = 6.821$, which intriguingly is yet another exact equality due to $\bar{a} = 1$. All the obtained results are summarized in Table I for easy comparison. It is evident that the observables for the black and wormhole are quite close, and some are exactly the same, giving strength to the idea that the Ellis-Bronnikov wormhole can act as a black hole mimicker within experimental accuracy.

This raises a very relevant question about the main observable and the current experimental accuracy, and how it can constrain γ. The central observable is the angular radius θ_∞ of the shadow of the object, which is primarily determined by its mass-to-distance ratio with a weak dependence on spin within the Kerr metric of the theory of general relativity. If the theory is violated, the shadow size may also depend strongly on parametric deviations from the Kerr metric. The result and uncertainty in θ_∞ from a simulated one-day observing run of the seven station EHT demonstrate that such an observation can measure θ_∞ of SgrA* with an uncertainty of 1.5 microarcsec (6%) [23]. (The possibility of directly imaging the shadow of the lens in the not-too-distant future is quite promising [12,43].) We calculated in Eq. (32) that the level of accuracy needed to distinguish between the Schwarzschild black hole and the Ellis-Bronnikov wormhole of the same mass and distance is 1.205 microarcsec. The plot of the difference function $\Delta(\gamma)$ of Eq. (33) then shows that the constraint is $\gamma \geq 80$ (Fig. 1).

A final remark: Despite intriguingly similar, even the same, observable values, it is our conviction that the Ellis-Bronnikov wormhole for real values of γ would survive as a topological object of its own class, remaining fundamentally distinct from a Schwarzschild black hole. This would be expected because a real $\gamma > 0$ cannot jump to $\gamma = -i$, augering a spontaneous topology change against experience [4,36]. By an intuitive extension, it is tempting to elevate this conviction into a principle: *Collapse of any object will lead to a final state definable only within the parameter range of the initial object and not to a state defined by parameters outside that range.*

APPENDIX: CALCULATION OF $\bar{b}$ FOR ELLIS-BRONNIKOV WORMHOLE

In the expression for $\alpha(\theta)$, θ is an independent angular variable designating different rays, and since $\bar{a} = 1$, the only quantities that can be expressed in terms of generic mass M are the minimum impact parameters u_m and $\bar{b}$. The u_m has already been expressed as such in Eq. (30). To obtain the functional expression for $\bar{b}$ in terms of M, it is necessary to briefly state its origin as developed by Bozza [11]. Thus the Ellis-Bronnikov metric is taken as [see Eq. (4)]

$$d\tau^2 = A(\ell)dt^2 - B(\ell)dr^2 - C(\ell)(d\theta^2 + \sin^2\theta d\varphi^2).$$

A photon incoming from infinity with arbitrary impact parameter u will be deviated while approaching the black hole. The light ray will reach the closest approach distance ℓ_0 and then emerge in another direction. The two distances are generically related by

$$u = \sqrt{\frac{C(\ell_0)}{A(\ell_0)}}.$$

The minimum impact parameter is

$$u_m = \sqrt{\frac{C(\ell_m)}{A(\ell_m)}}.$$

We shall be using the Ellis-Bronnikov metric functions (4) that yield

$$\ell_m = \ell_{\mathrm{ps}} = 2M = 2m_0\gamma.$$

The deflection angle

$$\alpha(\theta) = -\bar{a} \ln \left(\frac{\theta D_{\mathrm{OL}}}{u_m} - 1 \right) + \bar{b}$$

can be expressed in a mass-dependent form. We just cite here the expression [Eq. (37) from [11]]

$$\bar{b} = -\pi + b_R + \bar{a} \log \left(\frac{2\beta_m}{y_m} \right), \qquad y_m = A(\ell_m),$$

$$b_R = I_R(\ell_m) = \int_0^1 g(z, \ell_m)dz,$$

and β_m is an expression involving derivatives of metric functions [see Eq. (24) of [11]]. Omitting the detailed generic expressions for β_m and $g(z, \ell_m)$, we only report here the final expressions for b_R and $\frac{2\beta_m}{y_m}$ for the Ellis-Bronnikov wormhole in terms of M. The integrand $g(z, \ell_m)$ has a formidable expression that has been calculated and numerically integrated by using *Mathematica 9.1*. To explicitly show the mass dependence of $\bar{b}$, define

$$K_1 = \frac{\exp(-\pi\gamma)}{M} \left[\exp(\pi\gamma) - \exp\{2\gamma\tan^{-1}(2M)\} \right] \sqrt{(1 + 4M^2)/K_2},$$

$$K_2 = \exp[-\pi\gamma + 2\gamma\tan^{-1}(2M)],$$

$$K_3 = \exp \left[2\gamma \left\{ \tan^{-1}(2M) + \tan^{-1}\cot \left(\frac{\log K_2}{2\gamma} \right) \right\} \right],$$

$$K_4 = \ln \left[\exp(-\pi\gamma)\{(1 - z)\exp[2\gamma\tan^{-1}(2M)] + z\exp(\pi\gamma)\} \right],$$

$$K_5 = \frac{z}{\gamma^2} [\exp(-\pi\gamma) - \exp\{-2\gamma\}\tan^{-1}(2M)],$$

$$K_6 = z[4M^2 - 1 - 12M\gamma + 4\gamma^2]\exp(\pi\gamma) \\ + [8\gamma(\gamma - M) + z(1 - 4M^2 + 12M\gamma - 4\gamma^2)]\exp\{2\gamma\tan^{-1}(2M)\},$$

$$K_7 = \exp \left[2\gamma\tan^{-1}\cot \left(\frac{\log K_4}{2\gamma} \right) \right],$$

$$K_8 = (1 - z)\exp[2\gamma\tan^{-1}(2M)] + z\exp(\pi\gamma),$$

$$K_9 = \exp \left[-\pi\gamma - 2\gamma\tan^{-1}(2M) - 2\gamma\tan^{-1}\cot \left(\frac{\log K_4}{2\gamma} \right) \right],$$

$$K_{10} = (1 + 4M^2)[(z - 1)\exp\{2\gamma\tan^{-1}(2M)\} - z\exp(\pi\gamma)] \times \sin \left(\frac{K_4}{2\gamma} \right).$$

Then

$$g(z, \ell_m) \equiv g(z, M, \gamma) = K_1 \times \left(\frac{-2\sqrt{K_3}}{\sqrt{K_5 K_6}} + \frac{\sqrt{K_7 K_8}}{\sqrt{K_2 + K_9 K_{10}}} \right). \tag{A1}$$

We have verified that the numerical integration

$$b_R = \int_0^1 g(z, M, \gamma)dz \tag{A2}$$

does yield the Schwarzschild value (for $\gamma = -i$), $b_R = 0.9496$. Furthermore, it can be verified that

$$\log\left(\frac{2\beta_m}{y_m}\right) = \log\left[\frac{\exp\left[-4\gamma\tan^{-1}(2\gamma)\right]\left[\exp(\pi\gamma) - \exp\left\{2\gamma\tan^{-1}(2\gamma)\right\}\right]^2[1+4\gamma^2]}{2\gamma^2}\right]. \tag{A3}$$

This yields the exact Schwarzschild value (for $\gamma = -i$), $\log(\frac{2\beta_m}{y_m}) = \log 6 = 1.7917$. Collecting the results, one has $\bar{b}^{\mathrm{Sch}} = -\pi + b_R + \bar{a}\log(\frac{2\beta_m}{y_m}) = -0.4002$, just as in [11]. For the Ellis-Bronnikov wormhole, it was noted that the observable values rapidly saturate at $\gamma \gtrsim 80$, so at large real γ, it can be verified that, for the same mass as that of the black hole,

$$b_R = 0.8999,$$

$$\log\left(\frac{2\beta_m}{y_m}\right) = \log(5.905) = 1.7758,$$

$$\bar{b}^{\mathrm{EB}} = -\pi + b_R + \bar{a}\log\left(\frac{2\beta_m}{y_m}\right) = -0.4658. \tag{A4}$$

This value $\bar{b}^{\mathrm{EB}}$ was used in the text to calculate the separation of images $s^{\mathrm{EB}} = 0.0315$. Note that b_R is a result of a definite integral (A2) giving definite numerical values for black and wormhole cases, so $\bar{b}$ is independent of coordinate choices in each case.

---

[1] B. P. Abbott *et al.* (LIGO/Virgo Scientific Collaboration), Phys. Rev. Lett. **116**, 061102 (2016).

[2] B. P. Abbott *et al.* (LIGO/Virgo Scientific Collaboration), Phys. Rev. Lett. **116**, 221101 (2016).

[3] V. Cardoso, E. Franzin, and P. Pani, Phys. Rev. Lett. **116**, 171101 (2016); **117**, 089902(E) (2016).

[4] M. Visser, *Lorentzian Wormholes—From Einstein to Hawking* (AIP, New York, 1996).

[5] K. K. Nandi, B. Bhattacharjee, S. M. K. Alam, and J. Evans, Phys. Rev. D **57**, 823 (1998).

[6] V. Faraoni, F. Hammad, and S. D. Belknap-Keet, Phys. Rev. D **94**, 104019 (2016).

[7] H. G. Ellis, J. Math. Phys. (N.Y.) **14**, 104 (1973); **15**, 520(E) (1974).

[8] K. A. Bronnikov, Acta Phys. Pol. B **4**, 251 (1973).

[9] R. A. Konoplya and A. Zhidenko, J. Cosmol. Astropart. Phys. 12 (2016) 043.

[10] R. A. Konoplya and A. Zhidenko, Phys. Rev. D **81**, 124036 (2010).

[11] V. Bozza, Phys. Rev. D **66**, 103001 (2002).

[12] T. Lacroix and J. Silk, Astron. Astrophys. **554**, A36 (2013).

[13] S. Liu and F. Melia, Astrophys. J. **573**, L23 (2002).

[14] K. Kokkotas and B. Schmidt, Living Rev. Relativ. **2**, 2 (1999).

[15] E. Berti, V. Cardoso, and A. O. Starinets, Classical Quantum Gravity **26**, 163001 (2009).

[16] V. Cardoso, A. S. Miranda, E. Berti, H. Witek, and V. T. Zanchin, Phys. Rev. D **79**, 064016 (2009).

[17] I. Zh. Stefanov, S. S. Yazadjiev, and G. G. Gyulchev, Phys. Rev. Lett. **104**, 251103 (2010).

[18] K. K. Nandi, A. Islam, and J. Evans, Phys. Rev. D **55**, 2497 (1997).

[19] K. K. Nandi and Y.-Z. Zhang, Phys. Rev. D **70**, 044040 (2004).

[20] S. Weinberg, *Gravitation and Cosmology* (John Wiley & Sons, New York, 1972).

[21] C. R. Keeton and A. O. Petters, Phys. Rev. D **72**, 104006 (2005).

[22] J. Bodenner and C. M. Will, Am. J. Phys. **71**, 770 (2003).

[23] T. Johannsen, C. Wang, A. E. Broderick, S. S. Doeleman, V. L. Fish, A. Loeb, and D. Psaltis, Phys. Rev. Lett. **117**, 091101 (2016).

[24] D. Psaltis, Living Rev. Relativ. **11**, 9 (2008).

[25] V. Bozza, Phys. Rev. D **67**, 103006 (2003).

[26] K. K. Nandi, Y.-Z. Zhang, and A. V. Zakharov, Phys. Rev. D **74**, 024020 (2006).

[27] S. Iyer, Phys. Rev. D **35**, 3632 (1987).

[28] C. Armendáriz-Picón, Phys. Rev. D **65**, 104010 (2002).

[29] J. A. González, F. S. Guzmán, and O. Sarbach, Classical Quantum Gravity **26**, 015010 (2009).

[30] J. A. González, F. S. Guzmán, and O. Sarbach, Classical Quantum Gravity **26**, 015011 (2009).

[31] K. A. Bronnikov, R. A. Konoplya, and A. Zhidenko, Phys. Rev. D **86**, 024028 (2012).

[32] I. Booth, Can. J. Phys. **83**, 1073 (2005).

[33] R. M. Wald and V. Iyer, Phys. Rev. D **44**, R3719 (1991).

[34] I. D. Novikov and A. A. Shatskiy, J. Exp. Theor. Phys. **114**, 801 (2012).

[35] S. W. Hawking, Phys. Rev. D **37**, 904 (1988).

[36] K. A. Bronnikov and S. G. Rubin, *Lectures on Gravitation and Cosmology* (Moscow Engineering Physics Institute, Moscow, 2008).

[37] R. A. Konoplya and A. Zhidenko, Rev. Mod. Phys. **83**, 793 (2011).

[38] F. R. Tangherlini, Phys. Rev. A **12**, 139 (1975).

[39] K. K. Nandi, A. A. Potapov, R. N. Izmailov, A. Tamang, and J. C. Evans, Phys. Rev. D **93**, 104044 (2016).

[40] C. V. Vishveshwara, Nature (London) **227**, 936 (1970).

[41] C. B. M. H. Chirenti and L. Rezzolla, Classical Quantum Gravity **24**, 4191 (2007).

[42] C. B. M. H. Chirenti and L. Rezzolla, Phys. Rev. D **94**, 084016 (2016).

[43] A. Ricarte and J. Dexter, Mon. Not. R. Astron. Soc. **446**, 1973 (2015).